

Porous dendritic copper: an electrocatalyst for highly selective CO₂ reduction to formate in water/ionic liquid electrolyte

Supplementary Material

Experimental Section

Chemicals

All chemicals including 1-ethyl-3-methylimidazolium tetrafluoroborate (98%), [EMIM](BF₄), tetrabutylammonium tetrafluoroborate, n-Bu₄BF₄, (99%), CuSO₄·5H₂O (99.9%), H₂SO₄ 99.8% and CH₃CN (99.9%) were purchased from Sigma-Aldrich.

Methods

For the construction of the 3D Cu nanodendritic porous network, a solution of 0.2 M CuSO₄, 1.5 M H₂SO₄ was initially prepared. Then, a Cu plate electrode (1 cm²) was immersed into the solution and a current of 0.5 A was applied using a galvanostat. Under these conditions, intense H₂ bubbles were generated resulting in Cu deposition in the form of a porous structure.^{1,2,3}

Electrochemical measurements were performed in a three-electrode two-compartment cell using a Bio-logic SP300 potentiostat. Ag/AgCl/3M KCl (hereafter abbreviated as Ag/AgCl) was used as the reference electrode and placed in the same compartment as the working electrode. A platinum counter electrode was placed in a separate compartment connected by a glass-frit and filled with the electrolytic solution. The surface of the working electrode was 1 cm². All potential values are given versus the potential of the Fc⁺/Fc couple added as an internal standard to the solution after measurement. In MeCN (8% H₂O, 0.1M n-Bu₄BF₄): E_{1/2} (Fc⁺/Fc) = 0.42 V vs Ag/AgCl. In [EMIM](BF₄)/H₂O (92/8 v/v): E_{1/2} (Fc⁺/Fc) = 0.37V vs Ag/AgCl.

H₂ measurements were performed by gas chromatography on a Shimadzu GC-2014 equipped with a Quadrex column, a Thermal Conductivity Detector and using N₂ as a carrier gas. Carbon monoxide, methane and other volatile hydrocarbons from the gas phase were analyzed using a gas chromatograph (Shimadzu GC-2010) equipped with a methanizer, a flame induction detector (FID) and a shincarbon ST (Restek) column. Methanol was assayed

by gas chromatography (Shimadzu GC 2010) using an Rtx-1 column (Restek) and a flame induction detector (FID). Formate, oxalate and glyoxylate concentrations were determined by ionic exchange chromatography (883 Basic IC, Metrohm).

^{13}C -formic acid analysis was carried out by ^{13}C -NMR spectroscopy. Electrolysis using a modified Cu electrode was carried out in [EMIM](BF₄)/H₂O (92/8% v/v) under $^{13}\text{CO}_2$ saturation. After 2 h, formic acid was analyzed by ^{13}C -NMR spectroscopy after addition of 0.2 ml of CD₃CN to 0.8 ml of the electrolysis solution. A blank experiment with $^{12}\text{CO}_2$ was also carried out. For analysis of ^{13}CO a mass spectrometer was directly connected to the electrochemical cell during standard bulk electrolysis under $^{13}\text{CO}_2$ saturation. The gas reference was Argon (MW = 40). Gaseous products were then analyzed by mass spectrometry every third minute. Control experiments were also run: (i) electrolysis with an Argon-saturated solution; (ii) electrolysis saturation of non-labelled CO₂.

SEM images were acquired using a Hitachi S-4800 scanning electron microscope. TEM and HRTEM images were obtained on a JEM-2100F transmission electron microscope (JEOL, Japan) with an accelerating voltage of 200 kV.

The X-ray powder diffraction (XRD) patterns were recorded using an X'Pert Pro P analytical diffractometer equipped with either a Cu-K α radiation source ($\lambda_{\text{K}\alpha 1} = 1.540598 \text{ \AA}$, $\lambda_{\text{K}\alpha 2} = 1.544426 \text{ \AA}$) or a Co-K α radiation source ($\lambda_{\text{K}\alpha 1} = 1.78897 \text{ \AA}$, $\lambda_{\text{K}\alpha 2} = 1.79285 \text{ \AA}$) with an X'Celerator detector. Rietveld refinements²³ were performed with the Full Prof suite of programs.

Electrochemical diffusion surface area (A_{diff})

The Randles-Sevcik equation served to calculate A_{diff} , the diffusion surface area:¹

$$i_p = 2.69 \times 10^5 n^{3/2} D^{1/2} A_{\text{diff}} C v^{1/2} \quad (1)$$

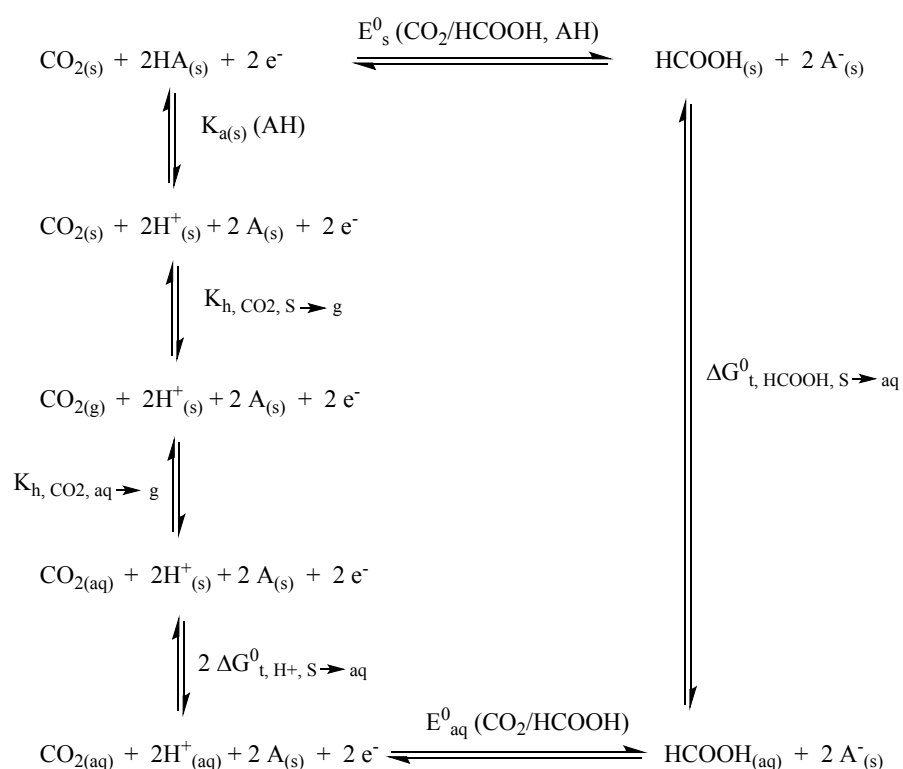
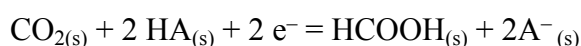
Here, i_p is the peak current corresponding to the reduction of redox species (Fe³⁺/Fe²⁺), obtained by CV of a K₃[Fe(CN)₆] solution, n is the number of exchanged electrons, D is the diffusion coefficient of the analyte ($7.5 \times 10^{-6} \text{ cm}^2 \text{ s}^{-1}$),¹ A_{diff} is the diffusional surface area, C (mol.cm⁻³) is the molar concentration of the analyte and v is the scan rate (V s⁻¹).

CV was recorded using either a Cu plate or a modified Cu electrode in 0.1M phosphate buffer pH 7.0 containing 5mM K₃[Fe(CN)₆] (scan rate 50mV.s⁻¹). Using the experimental i_p value from the CV, application of the equation above allowed the determination of the A_{diff} value.

Determination of the standard potential of the CO₂/HCOOH couple in CH₃CN

The method used below is directly taken from references ⁴ and ⁵ but we reproduce it in full for the sake of clarity. Of note however is the fact that we do not include the inter-liquid junction potential in the value of the standard potential of the CO₂/HCOOH couple versus NHE while we do it in a second stage when we refer it to the reference system used to measure electrochemical potentials.

We first determine the standard potential of the CO₂/HCOOH couple in a solvent S and in the presence of a weak acid AH referred to the aqueous normal hydrogen electrode (NHE). The redox half-reaction reads as follows:



Scheme S1

We use the thermodynamic cycle shown in Scheme S1 and derive the following equation

$$E_s^0(\text{CO}_2/\text{HCOOH}, \text{AH}) = E_{\text{aq}}^0(\text{CO}_2/\text{HCOOH}) -$$

$$\frac{RT \ln 10}{F} pK_{a(s)}(\text{AH}) - \frac{RT}{2F} \ln \left(\frac{K_{h, \text{CO}_2, \text{aq} \rightarrow \text{g}}}{K_{h, \text{CO}_2, \text{S} \rightarrow \text{g}}} \right) - \frac{2 \Delta G_{t, \text{H}^+, \text{S} \rightarrow \text{aq}}^0 - \Delta G_{t, \text{HCOOH}, \text{S} \rightarrow \text{aq}}^0}{2F}$$

with

$$E_{\text{aq}}^0(\text{CO}_2/\text{HCOOH}) = -0.11 \text{ V vs NHE at pH } 0^6$$

$$\Delta G_{t, \text{H}^+, \text{DMF} \rightarrow \text{aq}}^0 = -46 \text{ kJ/mol}_7$$

$$\Delta G_{t, \text{HCOOH}, \text{DMF} \rightarrow \text{aq}}^0 = -24 \text{ kJ/mol}_5$$

$$K_{h, \text{CO}_2, \text{S} \rightarrow \text{g}} = \frac{P_{\text{CO}_2} / P^0}{[\text{CO}_2]_{(\text{S})} / C^0}, \text{ with } [\text{CO}_2]_{(\text{S})} \text{ the solubility of } \text{CO}_2 \text{ in the solvent of interest under } P_{\text{CO}_2} = 10^5 \text{ Pa; } P^0 = 10^5 \text{ Pa and } C^0 = 1 \text{ mol.L}^{-1}$$

$$[\text{CO}_2]_{\text{CH}_3\text{CN}} = 0.28 \text{ mol.L}^{-1}^8 \text{ and } [\text{CO}_2]_{\text{aq}} = 0.038 \text{ mol.L}^{-1}^9$$

$$\text{We obtain } E_{\text{CH}_3\text{CN}}^0(\text{CO}_2/\text{HCOOH}, \text{AH}) = 0.216 \text{ V vs NHE} - \frac{RT \ln 10}{F} pK_{a(\text{S})}(\text{AH})$$

Considering now that H_2CO_3 formed by hydration of CO_2 is the strongest acid in the CO_2 -saturated CH_3CN and using the pK_a value of 17.03 previously determined for this couple in CH_3CN ,⁴ we finally obtain $E_{\text{CH}_3\text{CN}}^0(\text{CO}_2/\text{HCOOH}, \text{H}_2\text{CO}_3) = -0.79 \text{ V vs NHE}$.

To refer this potential versus the Fc^+/Fc couple, we use the experimentally determined value of $E(\text{Fc}^+/\text{Fc}) = 0.42 \text{ V vs Ag/AgCl/KCl } 3 \text{ mol.L}^{-1}$ ($E_{\text{Ag}/\text{AgCl}} = 0.210 \text{ V vs NHE}$) and correct it with the inter-liquid potential (0.100 V)¹ between the aqueous electrolyte of the Ag/AgCl electrode and the CH_3CN solution containing $n\text{-Bu}_4\text{BF}_4$ (0.1 mol.L⁻¹). This yields $E_{\text{CH}_3\text{CN}}(\text{Fc}^+/\text{Fc}) = 0.53 \text{ V vs NHE}$.

$$\text{Thus } E_{\text{CH}_3\text{CN}}^0(\text{CO}_2/\text{HCOOH}, \text{H}_2\text{CO}_3) = -1.32 \text{ V vs Fc}^+/\text{Fc}$$

Supporting Figures

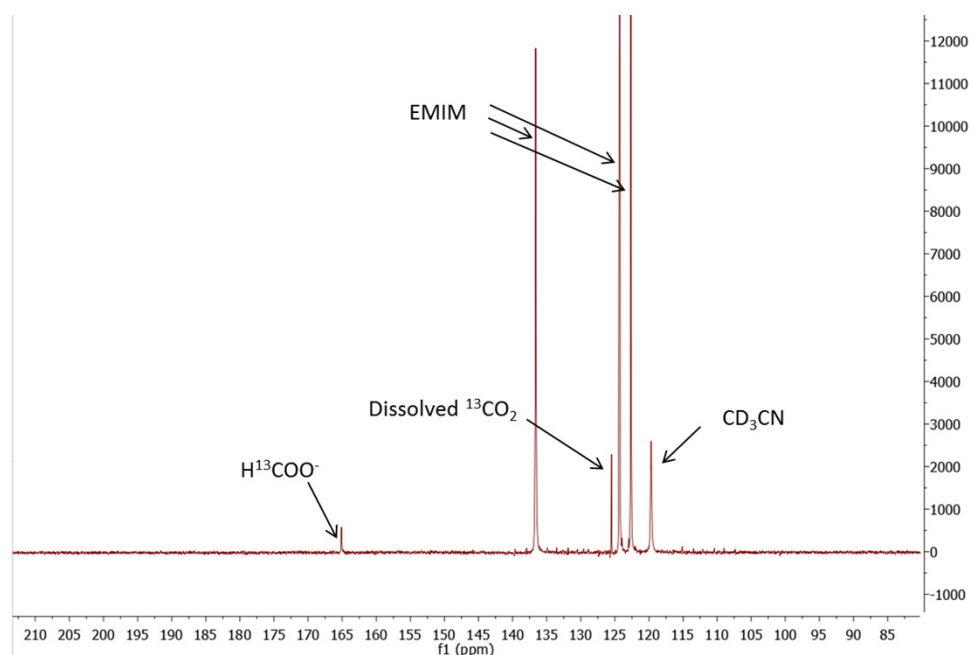


Figure S1: ^{13}C -NMR spectrum of an electrolytic solution using $^{13}\text{CO}_2$ reduction as the substrate in $[\text{EMIM}](\text{BF}_4)/\text{H}_2\text{O}$ (92/8 v/v) (0.8ml solution + 0.2ml CD_3CN). ^{13}C -formate is observed at 165 ppm.

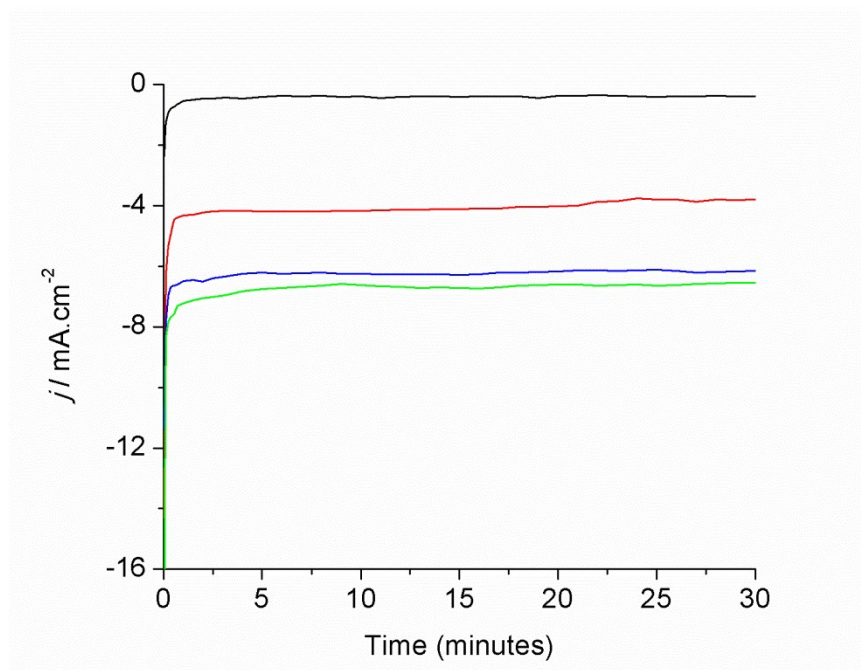


Figure S2: CPE at -1.55V vs Fc^+/Fc in $[\text{EMIM}](\text{BF}_4)/\text{H}_2\text{O}$ (92/8 v/v) at CO_2 saturation using the modified Cu electrode obtained after different electrodeposition times: 40s (red), 80s (blue), 120s (green). The modified Cu electrode (80s electrodeposition) was also used under N_2 (black).

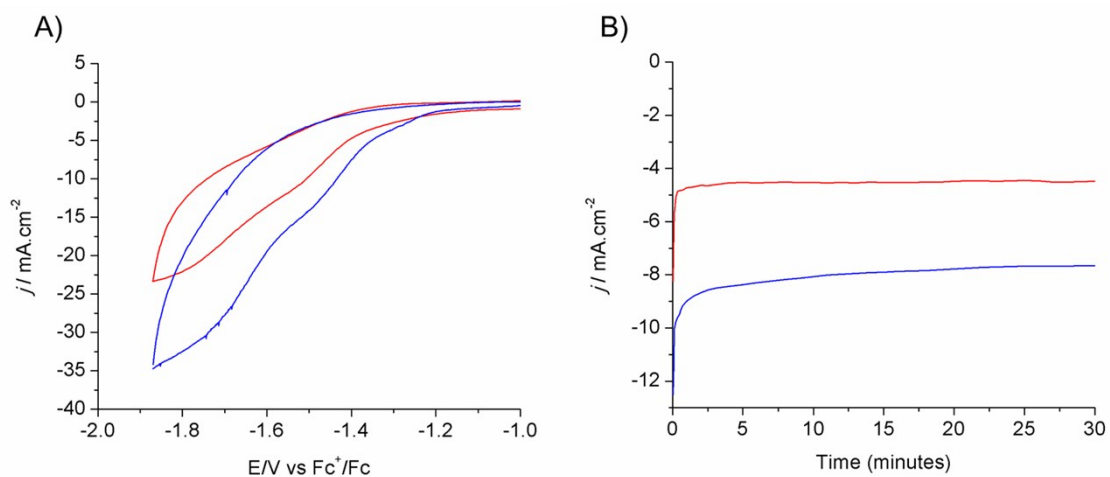


Figure S3: A) Cyclic voltammograms and B) current intensities during CPE using modified Cu electrodes obtained after different electrodeposition times (red: 40s; blue: 80s) in [EMIM](BF₄)/H₂O (85/15 v/v).

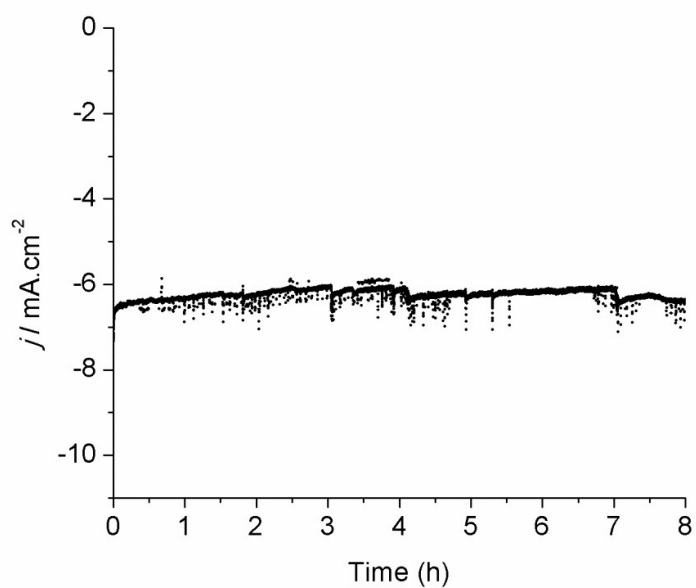


Figure S4: Catalytic current density during 8 h electro-reduction of CO₂ at -1.55 V vs Fc^+/Fc in [EMIM](BF₄)/H₂O (92/8% v/v) solution using a modified Cu electrode (80s electrodeposition).

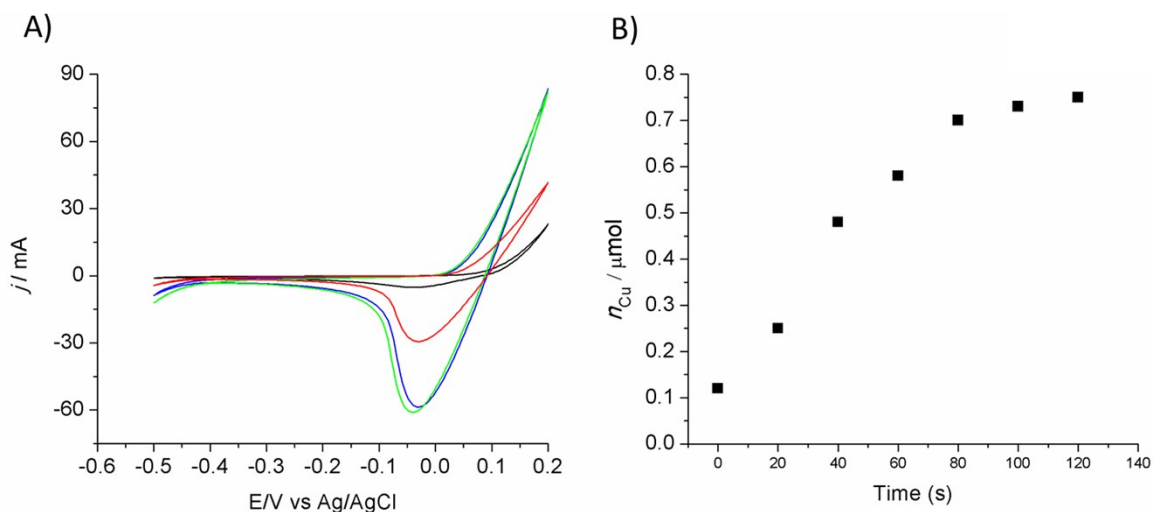


Figure S5: A) Cyclic voltammograms in H_2SO_4 0.5M using a Cu plate (black) or a modified Cu electrode (1 cm^2) obtained after 40s (red), 80s (blue) and 120s (green) electrodeposition. For sake of clarity the data for electrodes obtained after 20, 60 and 100 s are not shown. B) Surface concentration of active Cu calculated from the reduction peak in (A). From each CV total charge Q is calculated, and the amount of active Cu = $Q/(2 \times 1.6 \times 10^{-19} \times 6.02 \times 10^{23})$.

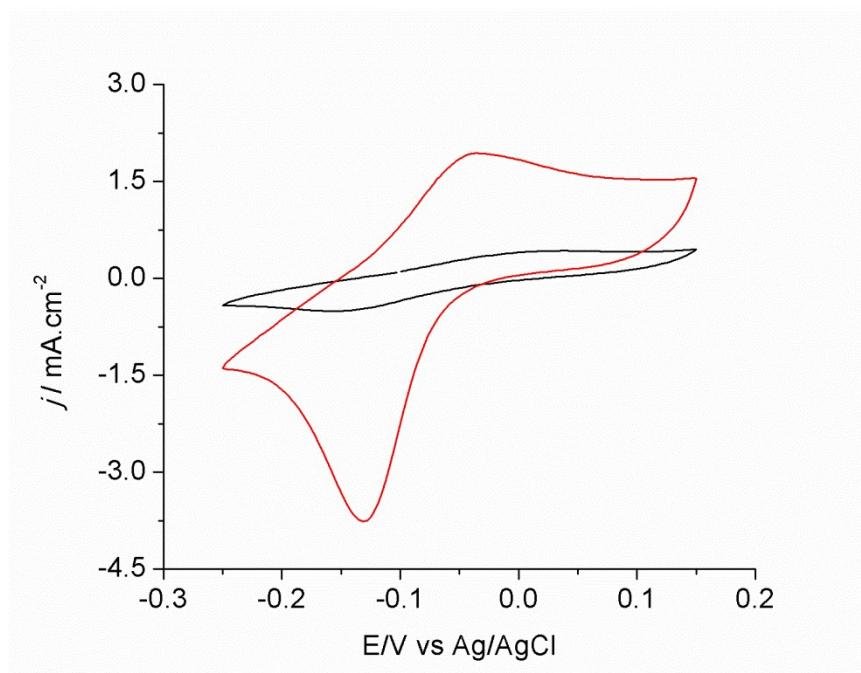


Figure S6: CVs of the Cu plate and the modified Cu electrode (80s deposition) in 0.1M phosphate buffer pH 7.0 containing 5mM $\text{K}_3[\text{Fe}(\text{CN})_6]$ (scan rate $50 \text{ mV}\cdot\text{s}^{-1}$).

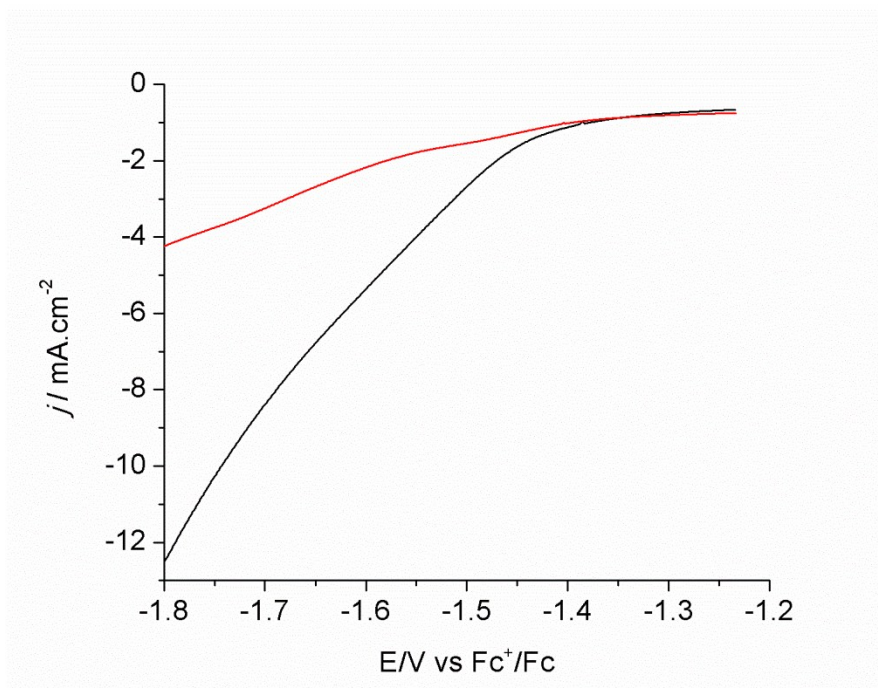


Figure S7: A) LSV of the modified Cu electrode (80s deposition) in MeCN/H₂O (92/8 v/v) + 0.1M n-Bu₄BF₄ under N₂- (red) and CO₂- (black) saturation conditions.

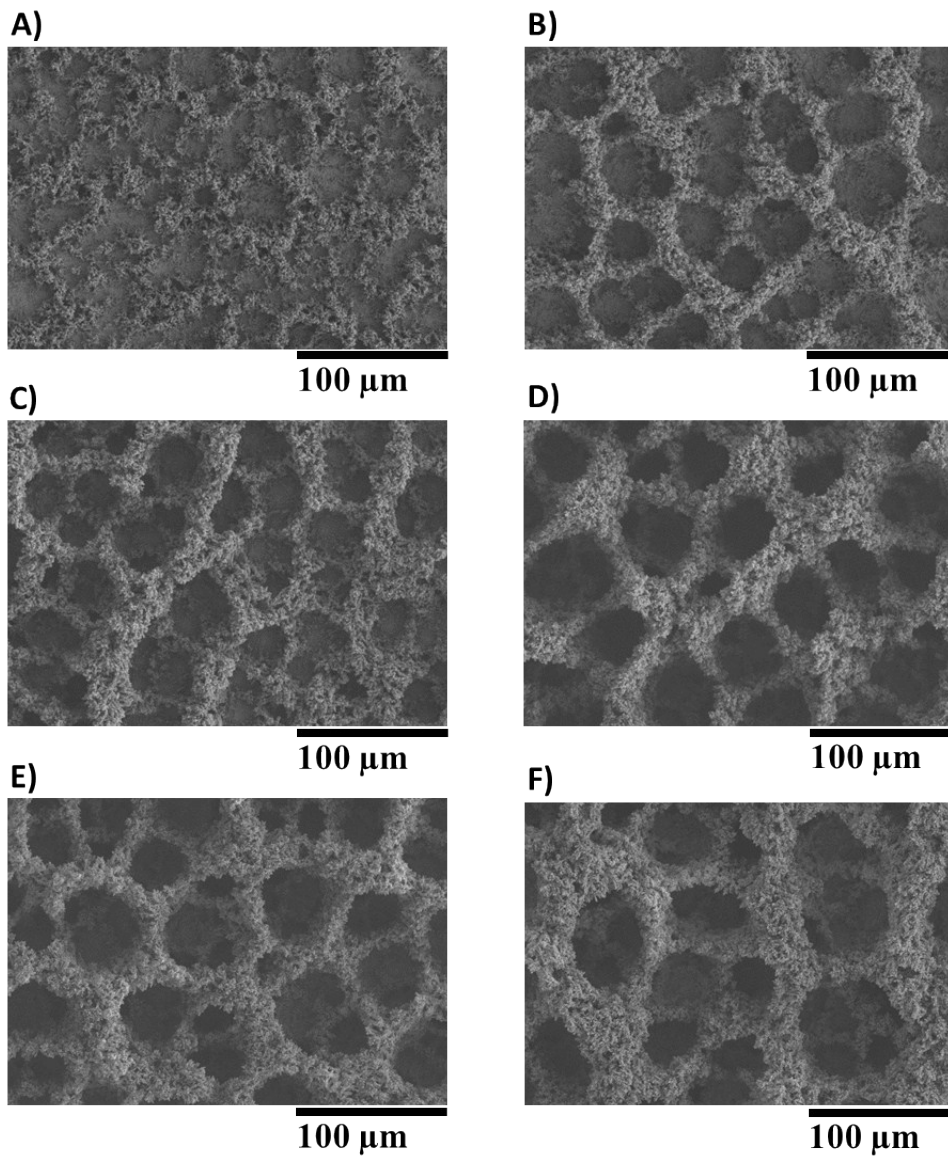


Figure S8: SEM images of the modified Cu electrodes obtained after 20s (A), 40s (B), 60s (C), 80s (D), 120s (E) and 160s (F) electrodeposition.

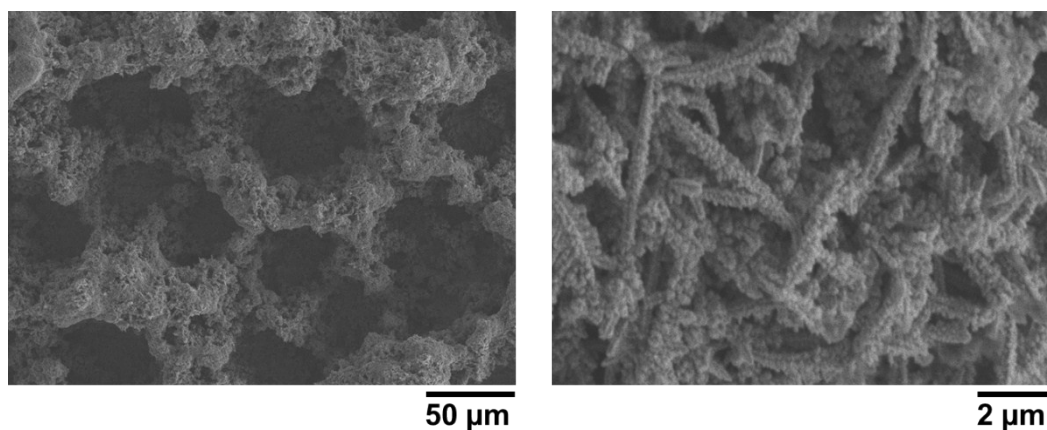


Figure S9: SEM image of the modified Cu electrode (80s electrodeposition) after long-term (8 h) electrolysis.

Table S1. Products and faradic yields during CPE at -1.55V vs Fc^+/Fc under CO_2 saturation in $[\text{EMIM}](\text{BF}_4)/\text{H}_2\text{O}$ (92/8 v/v) using a modified Cu electrode obtained after different electrodeposition times

| Electrodeposition time | Charge (C) | H_2 (%) | Formate (%) | CO (%) |
|------------------------|------------|------------------|-------------|--------|
| 40s | 5.8 | 9 | 82 | 5 |
| 80s | 8.6 | 8 | 83 | 5 |
| 120s | 9.1 | 11 | 79 | 6 |

Table S2: Products and faradic yields during CPE at -1.55 V vs Fc^+/Fc under CO_2 saturation in $[\text{EMIM}](\text{BF}_4)/\text{H}_2\text{O}$ (85/15 v/v) using modified Cu electrode obtained after different electrodeposition times.

| Electrodeposition time | Charge (C) | H_2 (%) | Formate (%) | CO (%) |
|------------------------|------------|------------------|-------------|--------|
| 40s | 10.2 | 35 | 50 | 8 |
| 80s | 16.8 | 36 | 49 | 9 |

References:

1. T.N. Huan, T.Ganesha, K.S. Kim, S. Kim, S.H. Han, H. Chung. *Biosens. Bioelectron.* **2011**, *27*, 183-186
2. H.C. Shin, M. Liu, *Chem. Mater.* **2004**, *16*, 5460-5464.
3. C. Zhu, D. Du, A. Eychmuller, Y. Lin, *Chem. Rev.* **2015**, *115*, 8896–8943.
4. C. Costentin, S. Drouet, M. Robert, J.M. Saveant, *Science* **2012**, *338*, 90-94.
5. T.N. Huan, E.S. Andreiadis, J. Heidkamp, P. Simon, E. Derat, S. Cobo, G. Royal, A. Bergmann, P. Strässer, H. Dau, V. Artero, M. Fontecave, *J. Mater. Chem. A* **2015**, *3*, 3901-3907.
6. T. Reda, C.M. Plugge, N.J. Abram, J. Hirst, *Proc. Natl. Acad. Sci. USA* **2008**, *105*, 10654-10658.
7. Y. Marcus, *Ion Properties* (Marcel Dekker, NY. 1997), p 216.
8. A. Gennaro, A.A. Isse, E. Vianello, *J. Electroanal. Chem.* **1990**, *289*, 203-215.
9. D.R. Lide, P.R. Frederikse, Eds. *Handbook of Chemistry and Physics*, (CRC Press, Boca Raton, FL, ed 76, 1995).